Supporting Information

Artemisinin: A novel Chiral Electrochemiluminescence Luminophore Assisted Enantiospecific Recognition and Mechanism Identification

Jiangyan Wang, ‡ Zhengang Han, ‡ Tianrui Shang, Yanjun Feng, Ruirui Liu, and Xiaoquan Lu*

Key Laboratory of Bioelectrochemistry and Environmental Analysis of Gansu Province,Key Laboratory of Water Security and Water Environment Protection in Plateau Intersection, Ministry of Education, College of Chemistry and Chemical Engineering, Northwest Normal University, Lanzhou, 730070, P. R. China.
‡ Jiangyan Wang and Zhengang Han contributed equally to this work.

Table of Contents

1. Materials and Instrumentation

Materials

Chemicals with analytical purity of KCl, K_2HPO_4, KH_2PO_4, potassium peroxydisulfate ($K_2S_2O_8$), ART, *L*-Cys, *D*-Cys were bought from Sinopharm Chemical Reagent Co., Ltd (Shanghai).

Instruments

The UV−vis spectra were recorded on an Agilent Cary 4000 spectrophotometer. Mass spectrum (ESI) data were recorded on a Shimadzu LCMS-2010EV mass spectrometer. pH values were obtained using a Mettler Toledo SevenMulti pH (S40) Meter (Switzerland). ECL was tested on ECL measurements using the MPI-E II ECL analyzer (Remex Electronic Instrument Ltd. Co., Xi'an, China). CV and DPV experiments in this work were performed using a CHI660 electrochemical workstation (Chenhua Instruments, Shanghai, China).

Experimental procedure

Before the electrochemical test, the glassy carbon electrode (GCE) was pretreated carefully. First, the electrode surface was cleaned with a lot of ultrapure water to remove the adsorbates. The electrode surface was then polished with an appropriate amount of 0.3 μM alumina. Subsequently, the polished electrode was characterized by cyclic voltammetry (0.2 ~ 0.6 V) in a 1.00 mM $K_3[Fe(CN)_6]$ solution. When the potential difference on the CV curve was less than 80 mV, the electrode treatment was proven to be successful.

The glassy carbon electrode is mainly composed of conductive carbon, and its preparation cost is relatively low. And it has good chemical stability, electrochemical performance, and biocompatibility. Due to the large surface area and sensitive electrochemical response of glassy carbon electrodes, they are widely used in the fields of biosensor research and electrochemical reactions. The Pt disk electrode can serve as an auxiliary electrode, mainly serving as a supplement to the research electrode, forming a polarization circuit that allows current to flow through the research electrode, while reducing the current density on the auxiliary electrode and minimizing the impact of polarization effects. However, the preparation process of Pt disks is relatively complex, and the cost of raw materials used is also high, so the preparation cost is relatively high. Moreover, Pt disks are mainly used for metal electrodeposition, electrochemical synthesis, and potential measurement. Therefore, in this work, GCE was used in the ECL experiment. A GCE has a diameter of 3 mm and an effective surface area of 2.25 mm^2.

Electrochemical and ECL measurements

ECL measurements were performed in 5mL PBS solution (100mM, pH = 7.4, containing a mixture of 0.1 M $K_2S_2O_8$ and 0.1 M (KCl, K_2HPO_4 and KH_2PO_4)) using an MPI-E II ECL analyzer. The potential range was -1.7 to 0 V, and the photomultiplier tube (PMT) was set to 800 V. After that, the ECL measurement was performed using a triangular potential scan with a scan rate of 200 mV/s. All electrochemical experiments were carried out through three electrode systems: a glass carbon electrode (GCE) with a diameter of 3 mm as the working electrode, platinum wire as the counter electrode, and Ag/AgCl as the reference electrode in saturated KCl solution. ECL spectra were collected using an Electrogenerated Chemiluminescence Spectrum System (Model ECLS-ML, FORTEC Technology (HK) Co. Ltd., Hong Kong, China) united with a CHI660 electrochemical workstation. Wavelength calibration was carried out by a mercury-argon lamp (Wyoptics, HG-1). And the obtained spectra were spooled together in a plot using graphing and analysis software of Origin.

0.1 M PBS solution (phosphate buffer solution, pH = 7.40) containing 100 mM $K_2S_2O_8$ and 4 μM ART was used as the electrolyte. For example, 20 μL of 1 mM ART was mixed with 5000 μL of 0.1 M PBS (pH 7.40) containing 100 mM $K_2S_2O_8$. The final concentration of ART was 4 μM. After that, the ECL measurement was performed using a triangular potential scan with a scan rate of 200 mV/s. A traditional three-electrode configuration was employed in this work, in which a glassy carbon electrode as the working electrode, an Ag/AgCl (saturated KCl) electrode as the reference electrode, and a Pt wire as the counter electrode were used.

SECM measurements

SECM measurements were operated at a UV–vis/SECM platform in a four-electrode system. The ultra-microelectrode is used as the working electrode, platinum wire serves as the auxiliary electrode, Ag/AgCl is used as the reference electrode, and a substrate film electrode sample is employed as the working electrode. The $K_3[Fe(CN)_6]$ (1 mM) was selected as a probe molecule.

2. Supporting figures

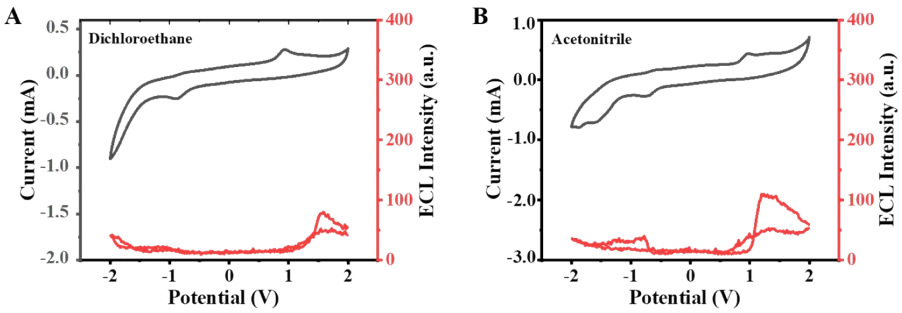

Fig. S1. Annihilation ECL.

The CV curve and annihilation ECL voltage curve of 1.0mM ART in dichloroethane (A) acetonitrile (B) solution, with 0.1M $TBPF_6$ as the supporting electrolyte. The scanning potential range is -2 to +2 V. The scanning rate is set to 0.2 V/s.

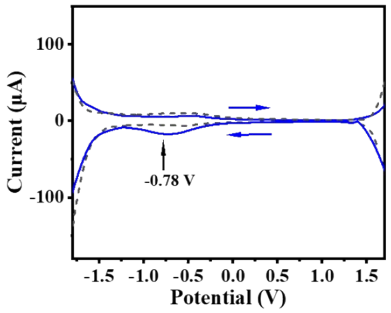

Fig. S2. Differential pulse voltammograms of ART modified GCE (blue) and bare GCE (black) in 0.1 M PBS (pH 7.4) solution.

The electroreduction behavior of ART was investigated using differential pulse voltammetry (DPV) in a preprepared PBS buffer solution with pH=7.4 (0.1 M KCl as the supporting electrolyte) and nitrogen saturated atmosphere. Under electrochemical conditions with a potential window of -1.7～1.7V and a scanning rate of 0.05V/s, compared to the bare glassy carbon electrode (GCE, black line), ART exhibits an irreversible reduction peak at around -0.8V, which is consistent with the CV results in Figure 2A.

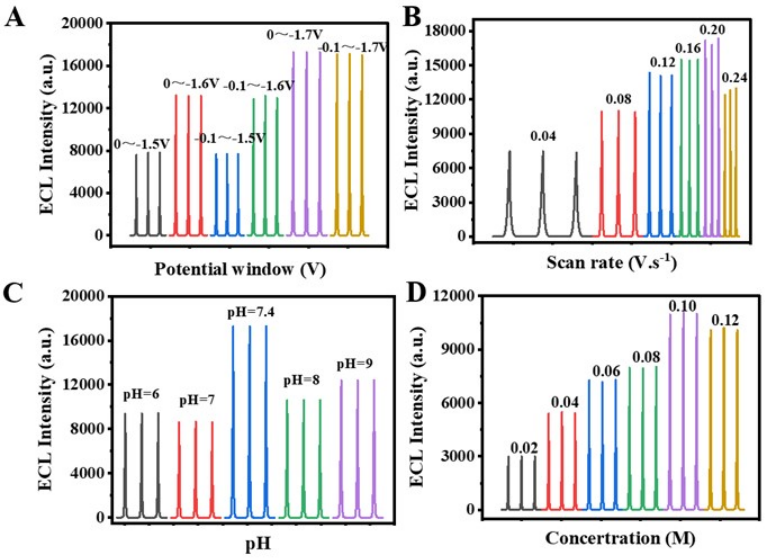

Fig. S3. ECL condition optimization.

(A) The influence of different pH values on the ECL intensity of ART. (B) The influence of $K_2S_2O_8$ concentration on the ECL intensity of ART. (C) The influence of different scanning rates on the ECL intensity of ART. (D) The influence of different potential windows on the ECL intensity of ART.

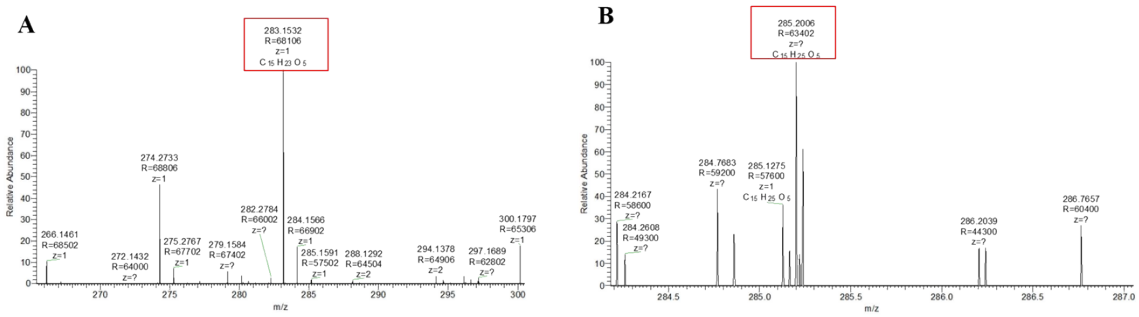

Fig. S4. Mass spectrum.

(A) The mass spectrum of ART. (B) The mass spectrum of ART after ECL test.

Fig. S4A shows the mass spectrum of ART. The theoretical mass-charge ratio calculated by mass spectrometry is 282.1462 and the actual mass-charge ratio calculated by mass spectrometry is 283.1532 $[M+H]^+$. Fig. S4B shows the mass spectrum of ART after ECL detection. The mass-charge ratio is 285.2006 $[M+H]^+$. These results show that during electroluminescence, the peroxo bond of ART is opened and two electrons are transferred, and then a protonation reaction occurs with hydrogen ions in solution.[1]

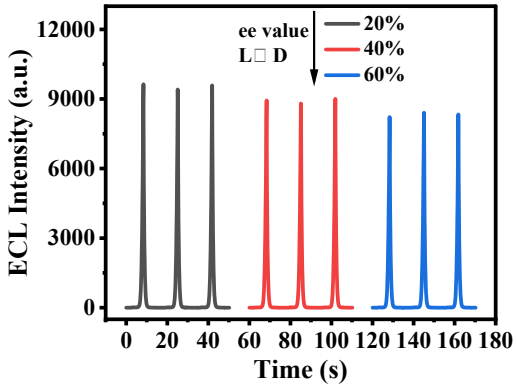

Fig. S5. ECL intensity-time curves of *D*/*L*-Cys mixtures with different enantiomer overpasses (20%, 40%, 60%) in ART-$K_2S_2O_8$ system.

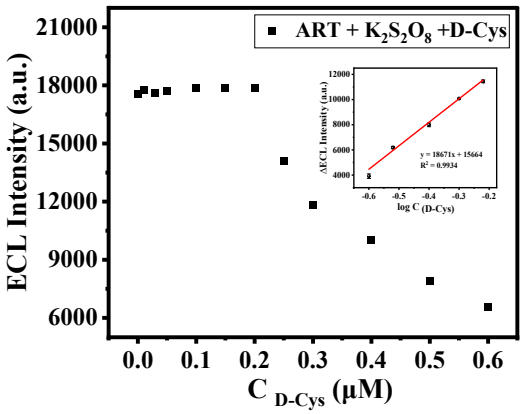

Fig. S6. ECL responses of the system at different *D*-Cys concentrations. The inset is Calibration curve.

There is a good linear relationship between the ECL intensity of artemisinin potassium persulfate system and the concentration of *L*-Cys in the range of 0.01-0.30 μM, but there is no linear relationship with *D*-Cys in this range. There is a linear relationship between the ECL intensity and *L*-Cys concentration of artemisinin potassium persulfate system in the range of 0.25-0.60 μM. Linear equation: $\Delta ECL=I_0-I=18671x+15664$, $R^2=0.9934$, where I_0 and I are the ECL strengths in the system without and with *D*-Cys, respectively. The calculated limit of detection (LOD) is 0.24 μM (S/N=3).

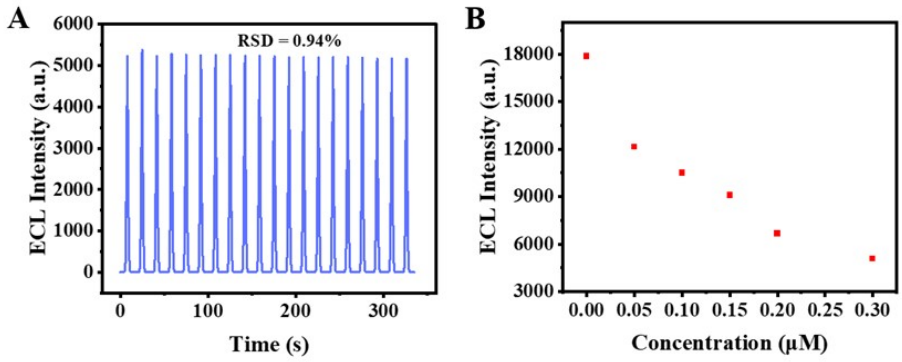

Fig. S7. (A) Stability of ART-$K_2S_2O_8$ system after adding 0.30 μM *L*-Cys to scan 20 cycles. (B) ECL sigals of 1 mM ART in 0.1 M PBS (pH=7.40) containing 0.1M $K_2S_2O_8$ with *L*-Cys (0.05 μM, 0.1 μM, 0.15 μM, 0.2 μM, 0.3 μM) in foetal bovine serum.

In general, the ECL detection of chiral cysteine was performed as following. At first, 20 μL ART was added into 5 mL PBS containing 0.1 M $K_2S_2O_8$. After scanning until ECL signal was stable, *L*-Cys of different concentrations (0, 0.01, 0.05, 0.10, 0.15, 0.20, 0.25, 0.30, 0.40, 0.50, 0.60 μM) were added into it respectively. The optimal experimental condition: a potential window: 0 V to -1.7 V (vs. Ag/AgCl), 200 mV/s scan rate, and pH = 7.4. Finally, the corresponding ECL intensity value vs each concentration was recorded for each test.

3. Supporting tables

Table S1. Comparison of ECL method with other reported methods.

Anaiyte	Methods	Linear range	LOD	Reference
L-Cys	fluorescence	0-100 μM	0.35 μM	2
	fluorescence	1.5-35μM	1.4 μM	3
	electrochemical	1-194 μM	0.617 μM	4
	electrochemical	1-10 μM	0.58 μM	5
	electrochemical	0.1-0.8 mM	12.8 μM	6
	electrochemical	0.001-2 mM	0.21 μM	7
	ECL	10-300 nM	3.7 nM	This work

Table S2. The rate constant K_{eff}.

Sample	ART	+ *L*-Cys	+ *D*-Cys
K_{eff} (10^{-2}cm/s)	0.66	0.60	0.49

4. Molecular Calculations

Using density functional (DFT) method, wb97xd/6-311++g(d, p) was used to optimize the geometric structure, and frequency verification was carried out. All the structures obtained were the lowest energy structures (using PCM continuum model considering solvation, the solvent was DMF). All calculations are done on the Gaussian16 program. The average local ion potential was calculated on Multiwfn 3.8 software.

References

1 A. M. Mugweru, A. Shore, H. K. Kahi, G. N. Kamau, *Int. J. Chem. Kinet*. 2016, **48**, 72−78.

2. Y. L. Xu, R. B. Bai, C. Y. Qi, Z. Ren, X. Z. Jia, Z. G. Kan, F. Wang, *J. Fluoresc*, 2019, **29**, 819−825.

3. X. Li, J. Qiao, Z. Li, L. Qi, *Anal. Chem*, 2020, **145**, 2233−2237.

4. T. Matsunaga, T. Kondo, I. Shitanda, Y. Hoshi, M. Itagaki, T. Tojo, M. Yuasa, *Carbon*, 2021, **173**, 395−402.

5. R. Jerome, P. V. Keerthivasan, N. Murugan, *Chemistryselect*, 2020, **5**, 9111−9118.

6. Y. Wang, W. Wang, S. Wang, *Sensor. Actuat. B-Chem*, 2016, **232**, 448−453.

7. J. Huang, F. Tao, Z. Sun, *Microchem. J*, 2022, **182**, 107915.